Acta Crystallographica Section A
Foundations of Crystallography
ISSN 0108-7673

Received 9 September 2011
Accepted 24 March 2012

Crystal-field effects in L-homoserine: multipoles *versus* quantum chemistry

B. Dittrich,[a,b]* E. Sze,[a] J. J. Holstein,[b] C. B. Hübschle[b] and D. Jayatilaka[a]*

[a]Chemistry, M313, School of Biomedical, Biomolecular and Chemical Sciences, University of Western Australia, Crawley, WA 6009, Australia, and [b]Institut für Anorganische Chemie der Universität Göttingen, Tammannstrasse 4, Göttingen, D-37077, Germany. Correspondence e-mail: bdittri@gwdg.de, dylan@theochem.uwa.edu.au

In contrast to an isolated molecule with identical geometry, the electron density of a molecule in the crystalline solid state is influenced by the field of surrounding molecules and by intermolecular hydrogen bonding. These influences have not yet found wide study on the level of the molecular electron-density distribution, which can be obtained both from high-resolution X-ray single-crystal diffraction as well as from *ab initio* quantum chemistry. To investigate this 'crystal-field effect' on the non-standard amino acid L-homoserine, three approaches were taken: (i) an *ab initio* point-charge isolated-molecule model; (ii) structure refinement with Hirshfeld atoms with and without surrounding point charges and dipoles; (iii) benchmark periodic calculations using density functional theory. For (i) and (iii) multipole models were fitted to static structure factors. The difference between the electron density obtained from the respective in-crystal model and from the isolated-molecular calculations yields detailed information on the crystal-field effect and dipole-moment enhancements. The point-charge model produces features of interaction density which are in good agreement with those from periodic *ab initio* quantum chemistry. On the other hand the multipole model is unable to reproduce fine details of the interaction density for zwitterionic homoserine.

1. Introduction

The polarizing effect of the crystal environment on the molecular electron-density distribution (EDD) is called the interaction density, *i.e.* the total electron density from which a sum of non-interacting molecular densities is subtracted. Our interest in interaction density is fuelled by its importance in the validation of theoretical approaches with experimental data and *vice versa*. An understanding of interaction density would enable us to improve current non-spherical scattering-factor databases derived from theory (Dittrich *et al.*, 2006; Dominiak *et al.*, 2007) in modelling experimental EDDs and to match the ability of the experimental ELMAM library (Zarychta *et al.*, 2007) to include the average influence of hydrogen bonding. Hence, prediction of crystal-field effects would be extended beyond the approximation of using gas-phase molecular electron density. While such improvements can be expected to play a minor role compared to improvements obtained when going from the independent-atom model to a non-spherical scattering model, any improvement in the accuracy of the scattering factors should be welcomed. Studies of interaction density might also contribute to our understanding of polarizations that take place during drug–receptor interactions or those in molecular recognition processes after the nucleation phase of the crystallization process.

The Hansen/Coppens modification (Hansen & Coppens, 1978) of the rigid pseudoatom formalism (Stewart, 1976) as used in current non-spherical refinement packages (order of the multipole expansion $l_{\max} = 4$ and one Slater-type radial function per shell with radial screening parameters κ) has been successfully used to analyse the EDD over the past decades (Tsirelson & Ozerov, 1996; Coppens, 1997; Koritsánszky & Coppens, 2001). However, it emerged that the model might not always be flexible enough to reproduce and describe fine electron-density rearrangements (Abramov *et al.*, 1999; Volkov *et al.*, 2000). An overriding situation is when rearrangements in the electron density due to crystal field and/or hydrogen bonding occur (interaction density), which has been investigated in a number of theoretical and experimental studies, *e.g.* on oxalic acid (Krijn *et al.*, 1988), urea, formamide (Gatti *et al.*, 1994; Spackman & Byrom, 1996) and sarcosine (Dittrich & Spackman, 2007), to name but a few. Based on the study of theoretical structure factors to which Gaussian noise was added, Krijn *et al.* (1988) were sceptical that the interaction density could be obtained from experimental data. On the other hand, Spackman & Byrom (1996) came to the opposite conclusion using unit-weight theoretical data. These findings led to ongoing efforts to develop the multipole model by increasing the flexibility of the radial functions used in the multipole model (Volkov & Coppens, 2001) or to increasing

the order l of the multipole expansion (Volkov *et al.*, 2009), which is especially important when the shell structure of metal atoms should be reproduced accurately. Unfortunately this increased flexibility reduces the data-to-parameter ratio which hampers the ability to obtain the interaction density from an experiment.

In contrast to multipole models, the flexibility of the basis functions is not an issue for quantum chemistry methods. However, quantum chemical codes are usually optimized for obtaining isolated-molecular properties, where geometries are obtained by energy minimization. To extract information on the interaction density, it is important not only to have flexibility in the basis functions, but to have accurate geometrical parameters.

Currently the most accurate solid-state geometries are obtained using Hirshfeld-atom refinement (Jayatilaka & Dittrich, 2008). This recent refinement method uses non-spherical scattering factors. They are generated from the molecular wavefunction obtained from a single-point self-consistent field (SCF) calculation. The resulting electron density is subdivided into atoms using Hirshfeld's stockholder partitioning (Hirshfeld, 1977). A Fourier transformation of the atomic electron density gives tailor-made scattering factors. We suggested the term 'Hirshfeld-atom structure refinement' (HAR) for least-squares refinement of positions and anisotropic displacement parameters (ADPs) including H atoms using these scattering factors (Jayatilaka & Dittrich, 2008) and will subsequently use this term in this work. The required functionality is implemented in the open-source program *TONTO* (Jayatilaka & Grimwood, 2003). Starting molecular geometries are obtained from a conventional spherical-atom refinement *e.g.* with *SHELXL* (Sheldrick, 2008), *CRYSTALS* (Betteridge *et al.*, 2003) or from invariom refinement (Dittrich *et al.*, 2005). The Hirshfeld refinement technique can also be performed with surrounding point charges and dipoles (again obtained from Hirshfeld partitioning) placed around a molecule. Although the geometrical and atomic displacement parameters are in excellent agreement with neutron diffraction data, the quality of the interaction density has not been investigated.

Herein, we are principally interested in two questions: firstly whether Hirshfeld-atom refinement with or without a field generated by a cluster of point charges and dipoles from Hirshfeld partitioning gives an accurate electron-density description; and secondly whether the multipole model is capable of achieving this. Periodic density functional theory (DFT) calculations are performed to provide a benchmark for both multipole and point-charge models. This study supersedes earlier work on sarcosine (Dittrich & Spackman, 2007) and uses the example of the non-standard amino acid L-homoserine.

2. Experimental data and model completion

The structure of L-homoserine was first determined by Chacko *et al.* (1982). A single crystal of the title compound [atom-numbering scheme depicted in an *ORTEP* representation (Burnett & Johnson, 1996) in Fig. 1] was grown by slow evaporation of an aqueous solution of the commercially obtained (Sigma Aldrich) compound. A single-crystal X-ray diffraction experiment was carried out at 100 K on an Oxford Diffraction 'Xcalibur S' diffractometer equipped with a nitrogen gas-stream cooling device. The software package *CrysAlis RED* (Oxford Diffraction, 2006) was used for data reduction and for a face-indexed analytical absorption correction (Clark & Reid, 1995). Good crystal quality and scattering power allowed measurement of data to a resolution of $\sin\theta/\lambda_{\max} = 1.19$ Å^{-1}. A data set with an overall coverage of 99.8% and an internal R factor of 3.8% was recorded over 4 d. No significant intensity decay was observed and the detector distance was 42 mm; every frame involved integration over a rotation of 1° in ω or φ. Crystallographic details can be found in Table 1 and in the cif/fcf files of the supplementary information.[1]

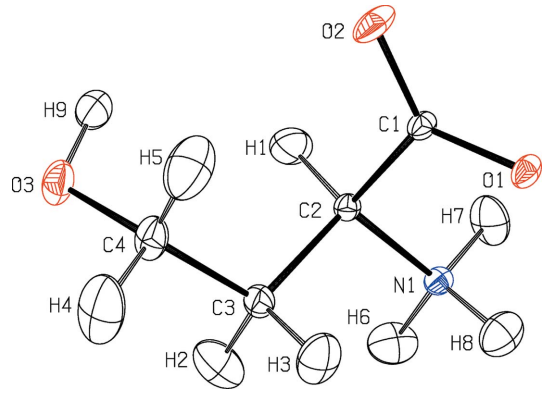

Figure 1
ORTEP representation (Burnett & Johnson, 1996) of the experimentally determined molecular structure in the crystal with the atom-numbering scheme and thermal ellipsoids with 50% probability. H-atom ADPs were estimated by the TLS + ONIOM method (for details see §2.2).

2.1. Preliminary refinements

Preliminary *SHELXL* structure refinement (Sheldrick, 2008) used the deposited coordinates from the entry BUHGOA (Chacko *et al.*, 1982) of the Cambridge Structural Database (CSD; Allen, 2002). Atoms were translated into the unit cell by shifting coordinates by $z + 1$. The original cell setting from Chacko *et al.* was kept; Friedel pairs were not merged. Subsequent non-spherical atom refinements with the invariom model (Dittrich *et al.*, 2004) gave non-H-atom ADPs and coordinates un-biased by bonding and lone-pair electron densities which are unaccounted for in the independent-atom model. Bond distances to H atoms were set to values from the invariom database (Dittrich *et al.*, 2006); model compounds as well as local atomic site symmetry used are given in the supplementary information.[1] The geometry thus obtained served as input for all following refinements and cluster

[1] Crystallographic details discussed in this paper are available from the IUCr electronic archives (Reference: WL5156). Services for accessing these data are described at the back of the journal.

calculations. An experimental multipole refinement was not performed. Hence, the high-resolution X-ray structure mainly provides accurate coordinates for our theoretical investigations.

A σ cutoff of $5.5\sigma(F)$ was chosen in our refinement with the 2003 version of *XDLSM* (Koritsánszky *et al.*, 2003).[2] It was found that introducing a second scale factor for all 201 reflections with $\sin\theta/\lambda \leq 0.35$ improved figures of merit and the Fourier residual-density maps – despite only showing a 3% difference in scale. Since the data are not used for refinement of multipole parameters, it was unproblematic to maintain the scaling in subsequent refinements. Differences in resolution-dependent scaling can be caused by a number of factors like absorption, extinction (not present here), thermal diffuse scattering and crystal quality. We will investigate the causes of such resolution-dependent scaling in more detail with suitable methodology in a subsequent paper.

2.2. Estimation of the anisotropic thermal motion of H atoms

An accurate description of the anisotropic thermal motion of H atoms is imperative for a study aiming to measure the fine details of EDD. Since a direct refinement of the ADPs of H atoms in L-homoserine by HAR led to imprecise results in terms of large standard deviations, we have estimated ADPs for H atoms following the TLS + ONIOM procedure (Whitten & Spackman, 2006). The H-atom ADPs thus obtained are required for obtaining the best possible H-atom positions in HAR. For that purpose the C code *BAERLAUCH* (Dittrich *et al.*, 2012) was used to generate a cluster of molecules starting from the fractional coordinates of the asymmetric unit content, taking into account space-group symmetry. In the next step a preliminary cluster of molecules was generated, including every molecule within a distance of 20 Å from the centre of mass of the first molecule. Ultimately every molecule containing an atom within a distance of 4.24 Å to any atom of the central molecule was included. This distance led to the generation of a cluster of 19 L-homoserine molecules with 323 atoms altogether, which in turn led to better SCF convergence compared to a cluster of 15 or 17 molecules. An ONIOM calculation (Svensson *et al.*, 1996; Dapprich *et al.*, 1999) was performed on the cluster. Only the central molecule was included in the high layer of the ONIOM calculation and it was geometry optimized at the DFT level of theory [functional/basis set: B3LYP/D95++(3df,3pd)], while all other molecules were part of the low layer as described by the universal force field UFF (Rappé *et al.*, 1992).

Low-layer atoms were not optimized. A representation of the cluster and the colour-coded symmetry operations of each molecule can be seen in Fig. 2. Having performed a geometry optimization in the cluster, we were able to compare also the optimized and experimental geometries, especially for bond distances involving H atoms. Potential-derived point charges (Besler *et al.*, 1990) were included in the calculation for the force-field atoms. They were derived from a preceding single-point energy calculation, again with the combination B3LYP/D95++(3df,3pd) of DFT functional and basis set. The converged geometry optimization in the cluster provided 'internal' infrared frequencies that were transformed into ADPs in the Cartesian crystal system with the *XDVIB1/2* programs of the *XD* package (Koritsánszky *et al.*, 2003), omitting the lowest six 'external' frequencies. In the TLS + ONIOM approach, these 'internal' contributions to the ADPs are subtracted from the experimental (refined in the presence of the aspherical electron density) ADPs of the non-H atoms. The remaining contributions to the ADPs were subsequently subjected to a rigid-body fit with the program *THMA11* (Schomaker & Trueblood, 1968, 1998). The rigid-body contribution of the heavy atoms not contaminated by the 'internal' modes was then added to the calculated internal modes for the H atoms in the crystal frame. The *ORTEP*

[2] This cutoff corresponds to a $3\sigma(F)$ cutoff in the program *TONTO* (Jayatilaka & Grimwood, 2003) and ensured that the same number of data was used in all our refinements.

Table 1
Crystal and structure refinement data for L-homoserine.

Empirical formula	$C_3H_9NO_3$
Formula weight (g mol^{-1})	119.12
Cell setting, space group	Orthorhombic, $P2_12_12_1$ (No. 19)
Z	4
Temperature (K)	100 (1)
Unit-cell dimensions (Å):	
a	9.1735 (1)
b	11.4736 (2)
c	5.4171 (1)
V (Å^3)	570.167 (16)
Calculated density (g cm^{-3})	1.388
$F(000)$	256.0
Crystal size (mm)	$0.29 \times 0.26 \times 0.25$
Crystal form, colour	Rectangle, colourless
Wavelength λ (Å)	0.7107
Absorption coefficient μ (mm^{-1})	0.12
Absorption correction	Face-indexed analytical
T_{min}/T_{max}	0.99/0.94
Max. θ (°)	57.78
$(\sin\theta/\lambda)_{max}$ (Å^{-1})	1.19
Measured, independent, observed reflections	53166, 8015, 6322
Criterion for observed reflections	$F > 5.5\sigma(F)$
Overall completeness	99.8%
Redundancy	6.63
Weighting scheme	Based on measured s.u.'s†
$R_{int}(F^2)$‡	0.038

For 'Number of parameters', the coordinates of H atoms were set to calculated positions with bond distances obtained from model compounds in invariom refinement. H-atom positions were refined in HAR; the basis set used for obtaining these values was cc-pVTZ.

	Invariom	HAR
Number of parameters	74	100
N_{ref}/N_{var}	85.6	63.2
$R(F)$ (%)	2.39	2.37
$R_w(F)$	1.56	1.48
χ^2		3.16
S‡	1.90	1.78
$\Delta\rho_{max}$, $\Delta\rho_{min}$ (e Å^{-3})	0.22, −0.25	

† $w = 1/\sigma^2$, $\chi^2 = 1/(n_o - m_{var})\sum(F_c - F_o)^2/\sigma^2$. ‡ $R_{int}(F^2) = \sum|F_o^2 - F_o^2(\text{mean})|/\sum F_o^2$, $R_w = (\sum|F_c| - |F_o|)/\sigma^2/\sum|F_o|/\sigma^2$, $R_1(F) = \sum||F_o| - |F_c||/\sum|F_o|$, $S = [\sum(||F_o| - k|F_c||^2)/(n_o - m_{var})]^{1/2}$.

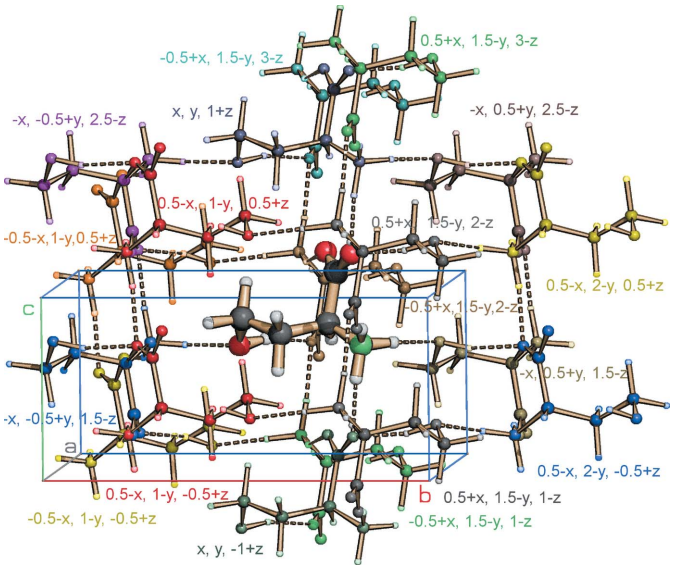

Figure 2
SCHAKAL99 (Keller & Pierrard, 1999) representation of the cluster used in the ONIOM calculation emphasizing the central molecule and including O—H···O and N—H···O hydrogen bonds.

(Burnett & Johnson, 1996) plot in Fig. 1 illustrates these estimated H-atom ADPs.

2.3. Hirshfeld-atom refinement

A HAR was then performed on the asymmetric unit content starting from the coordinates from invariom refinement. Positions and non-H-atom ADPs were adjusted by a least-squares minimization against the experimental data. The scattering factors used were derived from DZP (Dunning, 1970) and cc-pVTZ (Dunning, 1989) wavefunctions, which were obtained from a single-point energy calculation on the experimental geometry. To ensure convergence and the best possible fit, the procedure of SCF calculation, scattering-factor generation and least-squares fit were carried out over six iterations. The geometries obtained can be expected to optimally fit the basis set used. To estimate the crystal-field effect a parallel 'in-crystal' HAR included a field generated from dipole moments and atomic point charges surrounding the molecule to be optimized. A cluster radius of approximately 15 Å was employed, where charges and dipoles were obtained from Hirshfeld partitioning (Hirshfeld, 1977). This has been shown to improve the fit to experimental data (Jayatilaka & Dittrich, 2008). The difference density $\Delta\rho(\mathbf{r})$ between the isolated-molecular and the 'in-crystal' refinement will be discussed below in §3.3. Agreement factors for *XD* and *TONTO* refinements performed can be found in Table 1.

3. Results and discussion

HAR yields bond distances to H atoms in good agreement with theoretical predictions and neutron diffraction. This result is consistent with other implementations of structure refinement with non-spherical scattering factors (Dittrich *et al.*, 2005). Furthermore, ONIOM cluster calculations allow a comparison of bond distances of an optimized molecule in an environment approximating the solid state. As one can see from Table 2, even the trend in elongation of the hydrogen-bonded H atoms is reproduced, with for example the longer N—H bonds also being elongated in the cluster calculation. Despite recurrent claims to the contrary (Deringer *et al.*, 2012), accurate bond distances involving H atoms can hence indeed be obtained directly from X-ray diffraction using either Hirshfeld-atom or invariom refinement. Trends are also reproduced for other bond distances, *e.g.* those in the carboxylate group. However, having a shorter and a longer bond is still more pronounced in the experiment than in the ONIOM calculation. For comparison, we also report the elongated *X*—H bond distances from the invariom database as tabulated from DFT optimizations of model compounds with B3LYP/D95++(3df,3pd), which were used in invariom refinement and for generating the cluster.

Table 2
Bond distances (Å) from Hirshfeld-atom refinement (BLYP/cc-pVTZ) compared to a DFT ONIOM (B3LYP/cc-pVTZ:UFF) optimization of the central molecule in a 19-molecule cluster.

Optimized *X*—H bond distances from those invariom-database model compounds used in the refinement of homoserine are given for comparison.

Bond	Hirshfeld-atom refinement	ONIOM (B3LYP/cc-pVTZ:UFF)	Invariom database
O1—C1	1.2635 (3)	1.238	
O2—C1	1.2400 (3)	1.223	
O3—C4	1.4254 (4)	1.407	
O3—H9	0.968 (6)	0.972	0.961
N1—C1	1.4851 (3)	1.511	
N1—H6	1.020 (6)	1.027	1.023
N1—H7	1.016 (7)	1.010	1.023
N1—H8	1.062 (5)	1.037	1.023
C1—C2	1.5331 (4)	1.546	
C2—C3	1.5318 (3)	1.528	
C2—H1	1.088 (5)	1.072	1.101
C3—C4	1.5205 (4)	1.531	
C3—H2	1.074 (5)	1.084	1.094
C3—H3	1.101 (5)	1.087	1.094
C4—H4	1.075 (5)	1.081	1.096
C4—H5	1.090 (6)	1.080	1.096

3.1. Interaction density from periodic B3LYP calculations

One established method to study interaction density by theory is periodic Hartree–Fock (HF) or periodic DFT calculations (Spackman & Byrom, 1996; Dittrich & Spackman, 2007). The program *CRYSTAL06* (Dovesi *et al.*, 2008) was used to perform a single-point energy calculation with the functional/basis-set representation B3LYP/DZP for the experimental geometry. Experimental lattice constants were not optimized in the calculation. To smooth convergence, a level-shifting value of 0.6 Hartree for the molecular orbitals of the Fock matrix was specified. Interaction density features were first studied directly as obtained from the calculation. A difference density plot was obtained from two electron-density grids: the first grid was obtained with packed molecules, whereas in the second grid molecules were artificially

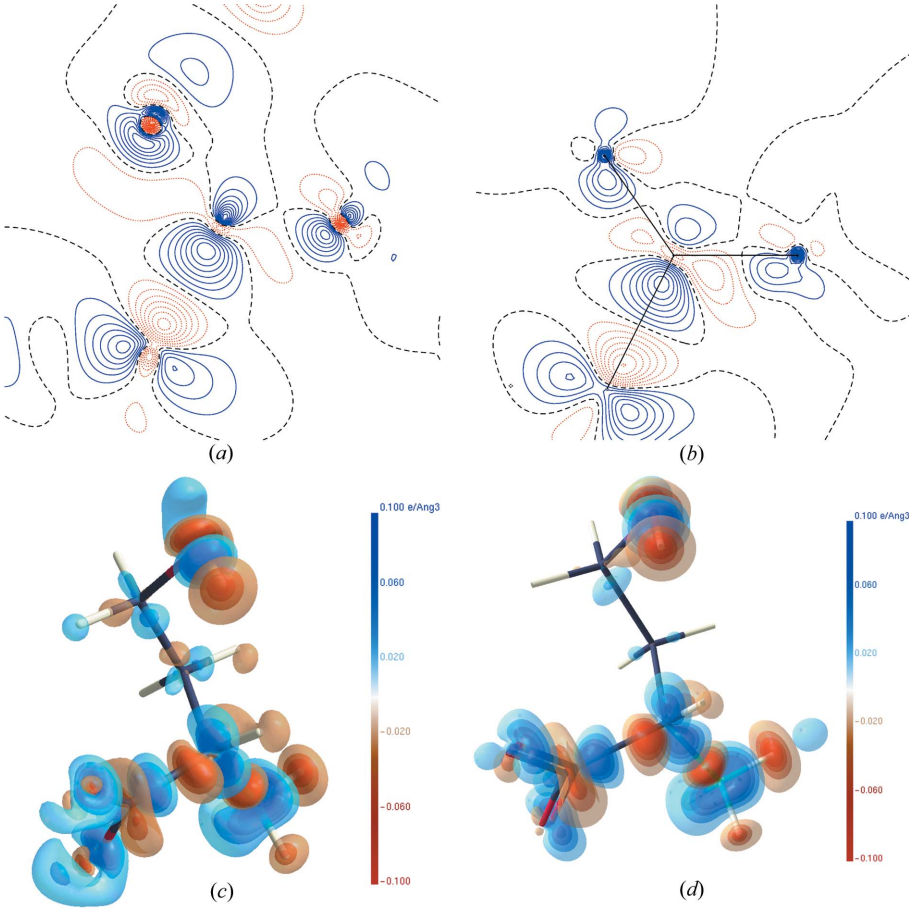

Figure 3
Two-dimensional interaction density of the C1O1O2 plane calculated from a periodic DFT calculation either obtained directly by comparing packed and artificially separated molecules ('molsplit' option) (*a*), or from a multipole model representation *via* generated structure factors (*b*). Additional density is depicted in different shades of blue, less density with respect to the isolated-molecular reference is shown in red. Contour lines are 0.025 e Å^{-3}. Three-dimensional plot directly from the calculation (*c*) with isosurface values of −0.025, −0.05, −0.075, −0.1, 0.025, 0.05, 0.075 and 0.1 e Å^{-3}; (*d*) shows the result from the multipole projection.

translated away from each other (maintaining the molecular geometry) so that no interaction remained. Such a procedure is evoked with the 'molsplit' option in the program *CRYSTAL06*.

The wavefunction was then evaluated to derive static theoretical structure factors. These were calculated both for the periodic calculation and the isolated molecule ('molsplit'). Both sets of structure factors were fitted with a multipole model. The fit was based on a model analogous to the one used in invariom refinement in both cases, except that atoms involved in hydrogen bonding were given more flexibility, *i.e.* by refining all multipoles for O atoms. To obtain an illustration of interaction density (see Fig. 3) a difference in the electron density $\Delta\rho(\mathbf{r})$ between the respective in-crystal molecule and the isolated molecule was calculated with the program *GRIDCON* (Whitten, 2006) that also performs grid conversions. Features seen in the basis-set representation (Fig. 3*a*) will serve as a benchmark for the following methodology. As an example, the C1O1O2 plane was chosen, whereas Fig. 3(*c*) depicts the difference density for the whole molecule. Contour plots were generated with *XDGRAPH* (Koritsánszky *et al.*, 2003) and three-dimensional representations with the program *MOLECOOLQT* (Hübschle & Dittrich, 2011). Features affecting covalent bonds are rather well reproduced by the multipole model projection, whereas electron density further away from the nuclei is not. Hence not all features can be faithfully reproduced by the projection onto the multipole model (Fig. 3*b*). The results of a Hartree–Fock calculation give a very similar result and are not shown. The lack of interaction density features in a multipole model description has implications for the recent research efforts to build a database of molecular fragments for use with (supposedly interacting) synthons in crystal engineering (Hathwar *et al.*, 2011). Since we find that such interactions are not well modelled in the multipole model, we think that there is no advantage over the scattering-factor databases introduced earlier.

While the basis-set size of periodic HF or DFT calculations can in principle be increased, there are intrinsic limitations with molecular basis sets. The choice of the DZP basis (Dunning, 1970) as recommended earlier (Spackman & Mitchell, 2001) should provide a reliable result. The effect of a more extended basis set will be investigated below in §3.3.

3.2. Interaction density from a simple point-charge model

A simpler model that allows the estimation of interaction density at low computational cost makes use of the potential-derived point charges mentioned earlier. The same DFT functional and basis set as in §2.2 was chosen. Point charges were placed at the same atomic positions that surround the central molecule depicted in Fig. 2, and used as input for the program *GAUSSIAN* (Frisch *et al.*, 2009). A single-point energy calculation of molecular electron density perturbed by a field of point charges was performed. The input file for *GAUSSIAN* was generated with the program *BAERLAUCH* (Dittrich *et al.*, 2012). Point charges obtained from the SCF calculation in the presence of charge perturbation were used as input in further single-point calculations with an updated set of potential-derived point charges until convergence. We have found that after the second iteration changes become small; after four cycles convergence to two significant figures was achieved. The

perturbed EDD was 'projected' on the same multipole model used above[3] in §3.1. Geometries were kept identical to the initial result from invariom refinement in both cases. After calculation of the electron density on a grid with *XDPROP*, a difference density generated with *ADDGRID* was calculated and is depicted in Fig. 4.

In analogy to the periodic calculation the result obtained directly from the basis-set representation can be compared to the multipole projection. Features seen for the latter are similar to the multipole-projected result from the periodic B3LYP calculation with *CRYSTAL06*. As before, Fig. 4(*a*) shows the C1O1O2 plane, whereas Fig. 4(*c*) depicts differences for the whole molecule. One can see that the more electronegative polar parts of the molecule are affected more strongly whereas the hydrophilic parts remain almost unaffected. The overall magnitude of the effect is small.

A variable input in this procedure is the cluster size. We have decided to maintain the cluster size that was sufficient to grant successful geometry optimization in the preceding ONIOM calculation as described in §2.2. We have also studied the influence of the cluster size on the difference density features. No significant changes were found for larger clusters than the one chosen for L-homoserine. However, smaller clusters than the one required to achieve convergence in the geometry optimization can probably not be considered sufficient to reproduce the crystal field. In summary we conclude that the point-charge model can provide a good estimate of the crystal-field effect at low computational cost.

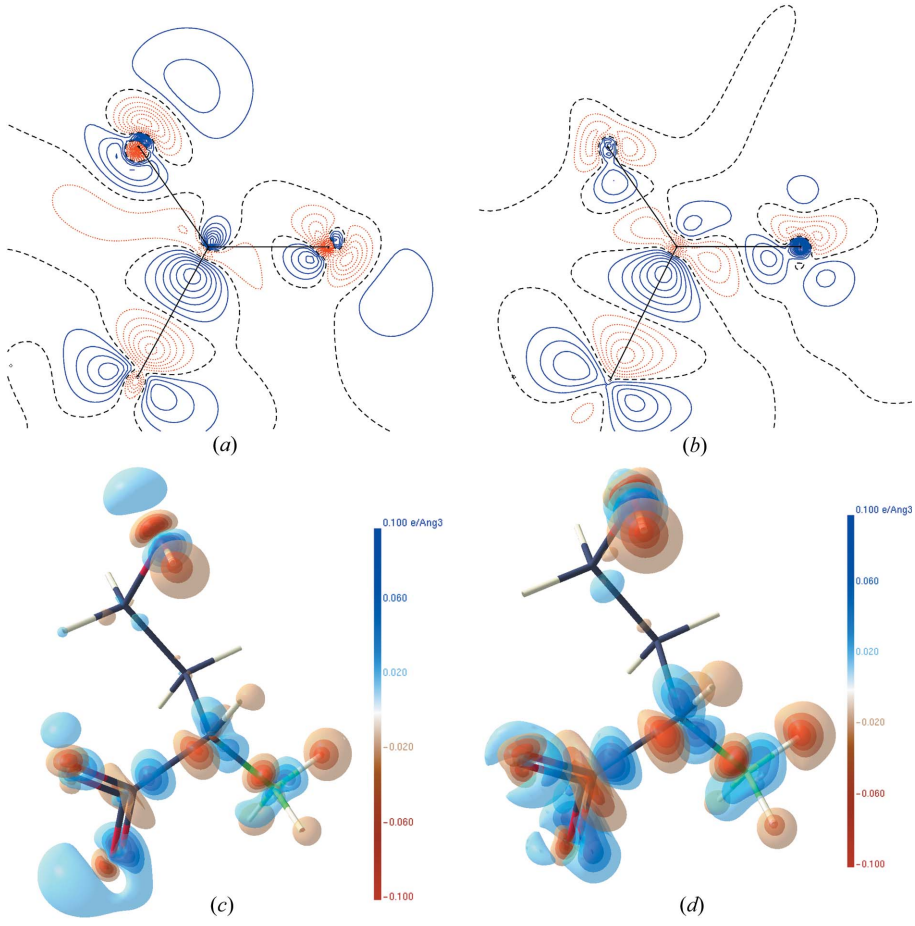

Figure 4
Two-dimensional interaction density calculated from a simple point-charge model directly from *GAUSSIAN09* for the carboxylate group (*a*), and for the whole molecule (*c*) in three-dimensional representation with contour levels and isosurface values chosen to be the same as in Fig. 3. (*b*) and (*d*) correspond to the same difference densities from the multipole model projection.

3.3. Interaction density from Hirshfeld-atom refinement with and without point charges and dipoles

Both calculations performed with *CRYSTAL06* and *GAUSSIAN09* relied on the geometry from invariom refinement, *i.e.* relying on the Hansen & Coppens (1978) multipole model. In Hirshfeld-atom refinement a possible influence of small geometric changes due to the basis-set flexibility on the interaction density can be excluded, since the structure is refined with the scattering factors obtained from the chosen basis set. Hence, HAR is best suited to study the influence of the basis-set size on the interaction density with the optimal experimental geometry. For that purpose we have refined a BLYP/DZP and a BLYP/cc-pVTZ geometry in the presence of point charges and dipoles with the program *TONTO*, giving an electron density on a grid. Subtracting the SCF density obtained in the absence of point charges and dipoles (but with the identical geometry) gave the two-dimensional and three-dimensional illustrations shown in Fig. 5. Features from the two basis sets do not differ much, with the cc-pVTZ basis being in principle capable of representing finer features of interaction density. One subtle difference from the earlier periodic calculations and the single-point calculations with *GAUSSIAN* is that for HAR with point charges and dipoles the radial expansion of the features around the carboxylate O atoms is more extended. Overall the agreement to the earlier basis-set models is excellent.

3.4. In-crystal dipole-moment enhancements

Theoretical studies, *e.g.* on urea and water (Gatti *et al.*, 1994), found an increase in the dipole moment in the solid state. However, a recent mini-review (Spackman *et al.*, 2007)

[3] The experimental resolution was used and the space group was $P\bar{1}$ with $a = b = c = 30$ Å. Further details of the procedure to 'project' the theoretical density onto the multipole model *via* 'simulated' structure factors were given previously (Dittrich *et al.*, 2005).

pointed out that dipole-moment determinations from experimental diffraction data using the Hansen and Coppens multipole model often report an exaggerated result. In Table 3 we list the results from our theoretical models. These are (i) the invariom refinement with fixed database multipoles, multipole projections of (ii) the *GAUSSIAN* point-charge model described in §3.2, (iii) the periodic *CRYSTAL06* B3LYP density, and finally two models based on Hirshfeld-atom refinement with/without a field of surrounding point charges/dipoles with different basis sets (iv) and (v). The point-charge model and Hirshfeld-atom refinement with point charges and dipoles give substantial in-crystal dipole-moment enhancements when compared to the two multipole projections. The slight enhancement of the dipole moment with the cc-pVTZ triple-ζ basis compared to DZP can be explained by cc-pVTZ having one more polarization function. Such polarization functions are not present in the *multipole projection* of the *CRYSTAL06* structure factors at all. Hence the enhancement cannot be modelled as well with the multipole model when compared to a basis-set description.

This interpretation is also consistent with the visual results obtained in §§3.1, 3.2 and 3.3. Since using point charges and dipoles in HAR improves figures of merit, geometries and ADPs (Jayatilaka & Dittrich, 2008), we think that they lead to a more realistic description of polarization, in contrast to the multipole model, which underestimates the effect. A good estimate of the dipole moment for a molecule in the in-crystal conformation can be obtained by invariom refinement at low computational cost.

Table 3
Dipole moments μ in Debye (D) for L-homoserine and enhancement in %.

The enhancement is $\%\Delta\mu = 100(\mu_{\rm mol@crystal} - \mu_{\rm mol})/\mu_{\rm mol}$ (Spackman *et al.*, 2007). (ii) is the result obtained using *GAUSSIAN*, (iii) is the result obtained using *CRYSTAL06*.

Method	μ (D)	Enhancement (%)
(i) Invariom refinement	11.2	
(ii) Isolated-molecular/point charges (multipole projection)	8.9/10.9	22.5
(iii) Isolated-molecular/in-crystal (multipole projection)	9.9/10.3	4.0
(iv) HAR† (DZP)	10.1/14.6†	44.6
(v) HAR† (cc-pVTZ)	9.7/14.8†	52.6

† Includes a surrounding field of point charges and dipoles within a 15 Å cluster.

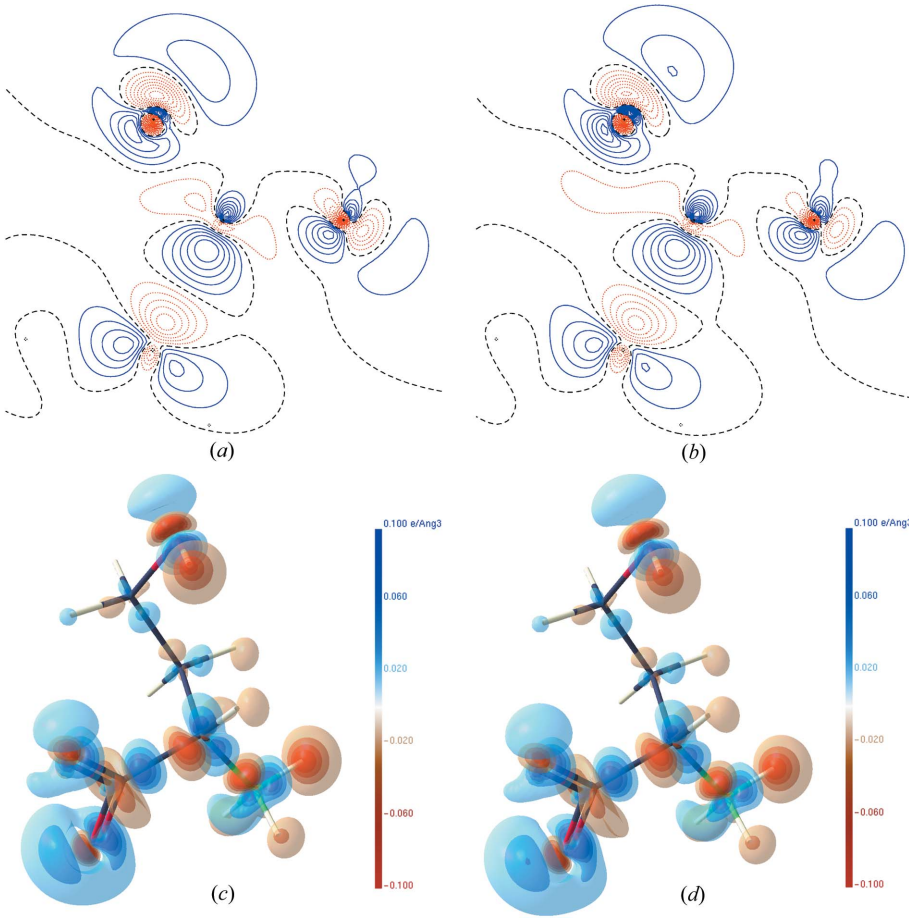

Figure 5
Two-dimensional (*a*) and three-dimensional (*c*) interaction densities from a difference between Hirshfeld-atom refinement including and not including a 15 Å cluster of point charges and dipoles using a DZP basis set. Contour levels and isosurface values are the same as in Fig. 4. (*b*) and (*d*) show similar results obtained from Dunnings cc-pVTZ basis set.

4. Conclusion

The crystal structure of L-homoserine was re-determined using invariom refinement and Hirshfeld-atom refinement with and without a cluster of surrounding point charges and dipoles. Using cluster charges and dipoles in HAR improves all figures of merit, indicating that a consistent geometry should be used within each methodology. The interaction density was obtained from three different methods, two point-charge models and a benchmark periodic B3LYP calculation. Both point-charge models showed almost indistinguishable interaction density features at the 0.025 e Å^{-3} level when compared to the periodic DFT benchmark. Moreover, the point-charge models required much less computational effort. Even the smaller 4.24 Å cluster with 19 molecules allowed us to reproduce features of the interaction density. A double-ζ basis was found to be already flexible enough to reproduce crystal-field effects. Clearly, for interaction densities of homoserine full periodic calculations are unnecessary. A multipole model projection was performed for the point-charge and periodic case. Although the *intra*-molecular features of the interaction density derived from the multipole

model are similar to periodic benchmark calculation, the *inter*-molecular interaction densities are not recoverable by the multipole model, at least using unit-weighted static structure factors up to the experimental resolution. A remaining question is to what extent an increase in data resolution can improve the ability of a modified multipole model to reproduce fine features of the electron density near the nuclei. It should also be noted that for van der Waals crystals, such as benzene, we would expect less perturbation than for the zwitterionic molecule with its strong hydrogen-bond network studied here. For homoserine, the embedded point-charge quantum mechanical basis-set representation is shown to be more accurate than the rigid-pseudoatom model for the electron density. The enhancement of the molecular dipole moment was also compared and shows some model and basis-set dependence.

Since flexible quantum mechanical methods for modelling and refining fine details of the interaction density of molecules from X-ray data are available today, it would seem expedient to focus on ensuring the quality of experimental data.

BD, JJH and CBH gratefully acknowledge funding from the Deutsche Forschungsgemeinschaft DFG for an Emmy Noether research fellowship, DI 921/3-1 and 3- 2. We thank Professor M. A. Spackman for support as well as diffractometer access in Perth, and J. Bak, P. Dominiak and K. Wozniak for helpful discussions.

References

Abramov, Y. A., Volkov, A. V. & Coppens, P. (1999). *Chem. Phys. Lett.* **311**, 81–86.

Allen, F. H. (2002). *Acta Cryst.* B**58**, 380–388.

Besler, B. H., Merz, K. M. & Kollman, P. A. (1990). *J. Comput. Chem.* **11**, 431–439.

Betteridge, P. W., Carruthers, J. R., Cooper, R. I., Prout, K. & Watkin, D. J. (2003). *J. Appl. Cryst.* **36**, 1487.

Burnett, M. N. & Johnson, C. K. (1996). *ORTEPIII*. Report ORNL-6895. Oak Ridge National Laboratory, Tennessee, USA.

Chacko, K. K., Swaminathan, S. & Veena, K. R. (1982). *Cryst. Struct. Commun.* **11**, p. 2037.

Clark, R. C. & Reid, J. S. (1995). *Acta Cryst.* A**51**, 887–897.

Coppens, P. (1997). *X-ray Charge Densities and Chemical Bonding.* No. 4 in IUCr Texts on Crystallography, 1st ed. Oxford University Press.

Dapprich, S., Komáromi, I., Byun, K. S., Morokuma, K. & Frisch, M. J. (1999). *J. Mol. Struct. (Theochem)*, **461**, 1–21.

Deringer, V. L., Hoepfner, V. & Dronskowski, R. (2012). *Cryst. Growth Des.* **12**, 1014–1021.

Dittrich, B., Hübschle, C. B., Luger, P. & Spackman, M. A. (2006). *Acta Cryst.* D**62**, 1325–1335.

Dittrich, B., Hübschle, C. B., Messerschmidt, M., Kalinowski, R., Girnt, D. & Luger, P. (2005). *Acta Cryst.* A**61**, 314–320.

Dittrich, B., Koritsánszky, T. & Luger, P. (2004). *Angew. Chem. Int. Ed.* **43**, 2718–2721.

Dittrich, B., Pfitzenreuter, S. & Hübschle, C. B. (2012). *Acta Cryst.* A**68**, 110–116.

Dittrich, B. & Spackman, M. A. (2007). *Acta Cryst.* A**63**, 426–436.

Dominiak, P. M., Volkov, A., Li, X., Messerschmidt, M. & Coppens, P. (2007). *J. Chem. Theory Comput.* **2**, 232–247.

Dovesi, R., Saunders, V. R., Roetti, C., Orlandol, R., Zicovich-Wilson, C. M., Pascale, F., Civalleri, B., Doll, K., Harrison, N. M., Bush, I. J., D'Arco, P. & Llunell, M. (2008). *CRYSTAL06*. Version 1.0.2. Universita di Torino, Torino, Italy.

Dunning, T. H. (1970). *J. Chem. Phys.* **53**, 2823–2833.

Dunning, T. H. (1989). *J. Chem. Phys.* **90**, 1007–1023.

Frisch, M. J. *et al.* (2009). *GAUSSIAN09*. Revision A.02. Tech. Rep. Gaussian Inc., Wallingford, CT, USA.

Gatti, C., Saunders, V. R. & Roetti, C. (1994). *J. Chem. Phys.* **101**, 10686–10696.

Hansen, N. K. & Coppens, P. (1978). *Acta Cryst.* A**34**, 909–921.

Hathwar, V. R., Thakur, T. S., Row, T. N. G. & Desiraju, G. R. (2011). *Cryst. Growth Des.* **11**, 616–623.

Hirshfeld, F. L. (1977). *Theor. Chim. Acta (Berl.)*, **44**, 129–138.

Hübschle, C. B. & Dittrich, B. (2011). *J. Appl. Cryst.* **44**, 238–240.

Jayatilaka, D. & Dittrich, B. (2008). *Acta Cryst.* A**64**, 383–393.

Jayatilaka, D. & Grimwood, D. J. (2003). *Computational Science – ICCS 2003*, *Lecture Notes in Computer Science*, Vol. 2660, edited by P. M. A. Sloot *et al.*, pp. 142–151. Melbourne, St Petersburg: Springer.

Keller, E. & Pierrard, J.-S. (1999). *SCHAKAL99*. University of Freiburg, Germany.

Koritsánszky, T. S. & Coppens, P. (2001). *Chem. Rev.* **101**, 1583–1628.

Koritsánszky, T., Richter, T., Macchi, P., Volkov, A., Gatti, C., Howard, S., Mallinson, P. R., Farrugia, L., Su, Z. W. & Hansen, N. K. (2003). *XD*. Freie Universität Berlin, Berlin, Germany.

Krijn, M. P. C. M., Graafsma, H. & Feil, D. (1988). *Acta Cryst.* B**44**, 609–616.

Oxford Diffraction (2006). *CrysAlis CCD and RED*. Version 1.171.31.5. Oxford Diffraction Ltd, Oxford, England.

Rappé, A. K., Casewit, C. J., Colwell, K. S., Goddard, W. A., Skid, W. M. & Bernstein, E. R. (1992). *J. Am. Chem. Soc.* **114**, 10024–10039.

Schomaker, V. & Trueblood, K. N. (1968). *Acta Cryst.* B**24**, 63–76.

Schomaker, V. & Trueblood, K. N. (1998). *Acta Cryst.* B**54**, 507–514.

Sheldrick, G. M. (2008). *Acta Cryst.* A**64**, 112–122.

Spackman, M. A. & Byrom, P. G. (1996). *Acta Cryst.* B**52**, 1023–1035.

Spackman, M. A. & Mitchell, A. S. (2001). *Phys. Chem. Chem. Phys.* **3**, 1518–1523.

Spackman, M. A., Munshi, P. & Dittrich, B. (2007). *ChemPhysChem*, **8**, 2051–2063.

Stewart, R. F. (1976). *Acta Cryst.* A**32**, 565–574.

Svensson, M., Humbel, S., Froese, R. D. J., Matsubara, T., Sieber, S. & Morokuma, K. (1996). *J. Phys. Chem.* **100**, 19357–19363.

Tsirelson, V. G. & Ozerov, R. P. (1996). *Electron Density and Bonding in Crystals. Principles, Theory and X-ray Diffraction Experiments in Solid State Physics and Chemistry*. Bristol, Philadelphia: Institute of Physics Publishing.

Volkov, A. & Coppens, P. (2001). *Acta Cryst.* A**57**, 395–405.

Volkov, A., Gatti, C., Abramov, Y. & Coppens, P. (2000). *Acta Cryst.* A**56**, 252–258.

Volkov, A., Koritsánszky, T., Chodkiewicz, M. & King, H. F. (2009). *J. Comput. Chem.* **30**, 1379–1391.

Whitten, A. E. (2006). *GRIDCON*. University of Western Australia, Crawley, Australia.

Whitten, A. E. & Spackman, M. A. (2006). *Acta Cryst.* B**62**, 875–888.

Zarychta, B., Pichon-Pesme, V., Guillot, B., Lecomte, C. & Jelsch, C. (2007). *Acta Cryst.* A**63**, 108–125.